RESEARCH ARTICLE

SPECIAL FOCUS: MICROFLUIDICS

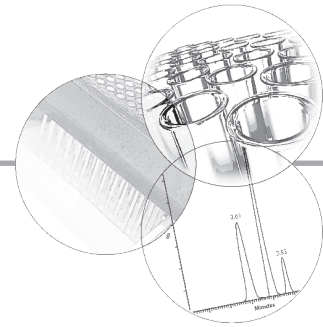

Transfection of molecular beacons in microchannels for single-cell gene-expression analysis

Background: Efficient transfection of molecular beacons has to be performed in the microscale in order to fully utilize the potential of molecular beacons and microfluidics for studying the real-time gene-expression dynamics in living cells. Nevertheless, there has been relatively little study on transfection of molecular beacons in microfluidic channels. **Results:** In this work, the differences between transfection in conventional cell culture systems and in microfluidic cell culture systems were investigated systematically with a combination of computational and experimental methods. Comparison between a no-flow microchannel and a 96-well plate revealed that the scale-dependence of reaction-diffusion kinetics contributes to the reduced transfection efficiency in the no-flow microchannel. Study on transfection in the microfluidic system under flow conditions suggested that the fluid flow enhances mass transfer, while the fluid shear stress can reduce the transfection efficiency. **Conclusion:** The results of this study will provide useful guidelines in optimizing molecular beacon transfection efficiency in microfluidic systems for studying gene-expression dynamics in living cells.

Na Li[†1] & Pak Kin Wong[2]

[1]Department of Mechanical & Aerospace Engineering, University of Miami, 1251 Memorial Drive, Coral Gables, FL 33124–0624, USA
[2]Department of Aerospace & Mechanical Engineering, Biomedical Engineering Interdisciplinary Program & Bio5 Institute, University of Arizona, Tucson, AZ 85721-0119, USA
[†]Author for correspondence:
Tel.: +1 305 284 3316
Fax: +1 305 284 2580
E-mail: n.li1@miami.edu

Cells actively respond to various internal or external stimuli by regulating gene expression associated with essential cellular processes such as proliferation, differentiation and signaling [1,2]. Both natural and artificial regulation of gene expression have been shown to be highly dynamic processes [3,4]. Therefore, the ability to dynamically monitor gene expression in living cells and to generate controllable cellular stimulation simultaneously is highly desirable for numerous biological and biomedical applications. To study the dynamic nature of cellular regulation, **molecular beacons** have been developed for monitoring gene expression at the transcriptional level [5]. The advent of microfluidics, on the other hand, has enabled new opportunities in studying cellular gene regulation by creating an *in vivo*-like cellular microenvironment [6] and generating controllable stimuli with high spatiotemporal precision [7,8].

Molecular beacons are fluorogenic oligonucleotide probes with a stem-and-loop structure for detecting specific nucleic acid sequences (**Figure 1**). In the molecular beacon design, the loop sequence is complementary to a specific sequence of a DNA/RNA target, and the stems are two complementary sequences at the two ends of the loop sequence. A fluorophore and a quencher are conjugated at the ends of the stem. When the molecular beacon self-hybridizes to form the stem–loop configuration, the fluorophore is in close proximity to the quencher, which causes the fluorophore to be quenched by the mechanism of the static quenching [9,10]. In the absence of the targeting DNA/RNA, the molecular beacon remains in the closed stem–loop configuration and does not fluoresce. In the presence of the targeting nucleic acids, the molecular beacon hybridizes to the target and forms a hybrid, which is thermodynamically more stable compared with the stem–loop configuration. This separates the fluorophore from the quencher, thus recovering the fluorescence. With proper design of the probe sequence, molecular beacons have been shown to be highly specific and sensitive [10–13]. The ability to homogeneously monitor nucleic acid targets with high sensitivity and specificity renders molecular beacons an excellent candidate for real-time monitoring of mRNA expression in living cells.

In addition to the molecular beacon, microfluidics provides novel tools for the investigation of cellular gene regulation. The small length of a microchannel creates a large surface-to-volume ratio and a small effective cell culture volume, which enhances gas transportation and creates a more *in vivo*-like culture environment [14,15]. Furthermore, proper length–scale matching between the cells and the microchannel allows the creation of various physical and biochemical

FUTURE SCIENCE part of fsg

Key terms

Molecular beacons: Fluorogenic oligonucleotide probes with a stem–loop structure.

Transfection: Intracellular delivery of nucleic acid compounds.

Electroporation: Method to introduce foreign materials to the cell by applying an electric pulse to temporarily disrupt the cell membrane.

stimuli with high spatiotemporal resolution and facilitates systematic investigation of the effects of these stimuli [16]. In order to utilize molecular beacons to study gene-expression dynamics in microfluidic systems, efficient **transfection** of molecular beacons has to be achieved in microfluidic systems. In conventional cell culture systems, transfection of nucleic acids can be performed by physical or chemical approaches. Physical methods, such as microinjection [17,18] and **electroporation** [19,20], involve temporary disruption of the cell membranes with physical stresses. The chemical methods, such as cationic lipids, cationic polymers [21–23] and translocation peptides [20,23,24], are to chemically modify the permeation properties of the nucleic acids. For microfluidics-based molecular beacon transfection, biochemical methods are preferred over physical methods to minimize the stresses on the cells and to transfect multiple cells simultaneously.

Transfection of molecular beacons has been successfully demonstrated in various live cell studies; however, relatively little is known about transfection of molecular beacons in microfluidic channels. The small effective cell culture volume in microfluidics could impact the effective concentration of molecular beacons for transfection, and the optimal transfection conditions in cell culture dishes might not be applicable to microfluidic cell culture systems. Furthermore, the shear stress induced by the fluid flow in the microchannel may influence the transfection efficiency of molecular beacons. In this work, the differences between transfection in traditional and microfluidic cell culture systems were investigated. A molecular beacon design was first characterized. Then, the effects of length–scale and fluid-flow were investigated systematically with a combination of computational and experimental methods. The roles of the effective concentration of the molecular beacon and the reaction-diffusion kinetics in microfluidic-based molecular beacons transfection are characterized. The study will serve as an example for the design of microfluidics-based gene expression analysis experiments using molecular beacons in the future.

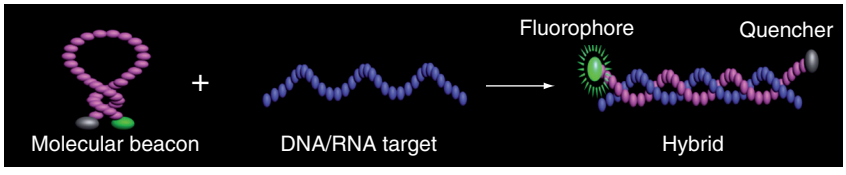

Figure 1. Molecular beacons.

Experimental

■ Materials

All oligonucleotides used in the experiments **(TABLE 1)** were synthesized by Integrated DNA Technologies (Coralville, IA, USA). Upon receipt, the oligonucleotides were dissolved with 1X TE buffer and then stored in aliquots at -20°C. The polydimethylsiloxane (PDMS) base polymer and curing agent were purchased from Dow Corning (Midland, MI, USA). SU-8 photoresist was obtained from MicroChem Corp (Newton, MA, USA). Cell culture media, fetal calf serum (FBS), penicillin/streptomycin (P/S) and L-glutamine were purchased from Invitrogen (Carlsbad, CA, USA). Transfection reagents JetPEI™ and Lipofectamine™ 2000 were purchased from Polyplus-transfection (New York, NY, USA) and Invitrogen, respectively. Unless otherwise specified, all other reagents were purchased from Sigma-Aldrich (St Louis, MO, USA).

■ Characterization of molecular beacons

A 2′-*O*-methyl molecular beacon targeting human β-actin mRNA (Actin MB) was used in all the transfection experiments. To verify the design of Actin MB, two synthetic oligonucleotide targets perfectly (ACTB) and partially (ACTB-1M) complementary to the loop region of Actin MB were designed. The sequence of the molecular beacon and the synthetic targets are shown in **TABLE 1**. In the experiment, 0.2 µM Actin MB and ACTB or ACTB-1M were preannealed in 50 mM KCl, 5 mM $MgCl_2$ and 10 mM Tris (pH 8.0) at 95°C for 5 min, and then slowly cooled to room temperature. A total of 40 µl of each preannealed mixture was added into a 96-well PCR plate. The thermal denaturation experiment of these solutions was conducted with an iCycler iQ™ real-time PCR system (Bio-Rad Laboratories, Hercules, CA, USA). The temperature was increased from 32 to 90°C at 1°C per step and the fluorescent intensity was measured after 1 min thermal equilibration at each step.

■ Microfluidic cell culture system

The microchannel was fabricated by micromolding of PDMS from an SU-8 photoresist master. The PDMS base polymer and curing agent were first mixed at a ratio of 10:1 and then degassed in a vacuum chamber for 10 min before pouring on the SU-8 master. After curing at 60°C for 2 h, the PDMS replica was carefully peeled off from the master and then irreversibly sealed

with a glass coverslip, immediately after exposing in oxygen plasma for 1 min (Harrick Plasma, Ithaca, NY, USA). A reservoir and a fluid outlet were bonded on top of the PDMS channel. The fluid outlet was connected to a peristaltic pump (Instech Laboratories, Plymouth Meeting, PA, USA), which was controlled by a Labview interface (National Instruments, Austin, TX, USA). The microchannel was sterilized by 70% ethanol and treated with 50 µg/ml fibronectin to promote cell adhesion before the experiment. The microchannel was loaded inside of a temperature controlled chamber (Instech Laboratories) that was maintained at 37°C for the duration of the experiment. In order to facilitate the real-time monitoring of the experiment, the heating chamber was installed on the stage of an inverted fluorescence microscope (Nikon TE200) equipped with a 1024×1024 pixel, 16-bit cooled Photometric CH350L CCD camera (Photometric, Tucson, AZ, USA). The entire setup **(FIGURE 2)** was located in a vertical clean bench to minimize the possibility of contamination.

■ Cell culture & transfection

Human embryonic kidney (HEK) 293T cells were used in the no-flow microchannel. Due to the poor adhesion of 293T cells, HeLa cells were used in the microchannel with flow. Both 293T and HeLa cells were cultured in Dulbecco's Modified Eagle's Medium (DMEM), supplemented with 10% FBS and 1% P/S. The day before the transfection experiment, the cells were seeded at 30–40% confluency in the microchannel. CO_2-independent cell culture media supplemented with 10% FBS, 1% P/S and 4 mM L-glutamine were used to eliminate the need for controlling the CO_2 level inside the heating chamber. On the day of transfection, the cells reached 60–80% confluency. Transfection reagents JetPEI™ and Lipofectamine™ 2000 were used for 293T and HeLa cells, respectively. The transfection reagents were mixed with molecular beacons according to manufacturer's instructions, and the mixtures were then added to the cell culture media.

Computational modeling

Two transfection reagents were used in the experimental study: the cationic linear polymer JetPEI™ and the cationic lipid Lipofectamine™ 2000. It has been shown that the transfection mechanisms for both reagents are similar: complexes formed by transfection reagents and DNA enter the cell by endocytosis [25,26]. Endocytosis

Table 1. Sequences of actin MB, ACTB & ACTB-1M (5'→3').

Actin MB	6-FAM/*CCCGA* GCGGCGAUAUCAUCAUCCAU *UCGGG*/Dabcyl†
ACTB	ATGGATGATGATATCGCCGC
ACTB-1M	ATGGTTGATGATATCGCCGC‡

†In Actin MB, all the nucleotides are 2′-O-methyl RNA nucleotides. Italics represent the complementary stems and normal fonts represent the loop.
‡The mismatched nucleotide is underlined.
6-FAM: 6-carboxyfluorescein; Dabcyl: 4-(dimethylaminoazo)benzene-4-carboxylic acid.

of these complexes can be divided into three steps: binding to cell surface, internalization by the cells and escape from endosome. The binding of the complexes to the cell surface is often the slowest, limiting step in this endocytic cycle and the binding reaction is assumed to be irreversible in our simulation. Under the above assumptions, the transfection was considered as a pseudo first-order reaction where the transfection rate was proportional to the concentration of transfection reagent/molecular beacon (T/M) complexes at the cell surface.

■ Computational model for transfection in the no-flow systems

For transfection in a no-flow system, the diffusion-reaction kinetics should be considered to estimate the local concentration of T/M complexes near the cell surface available for transfection. To

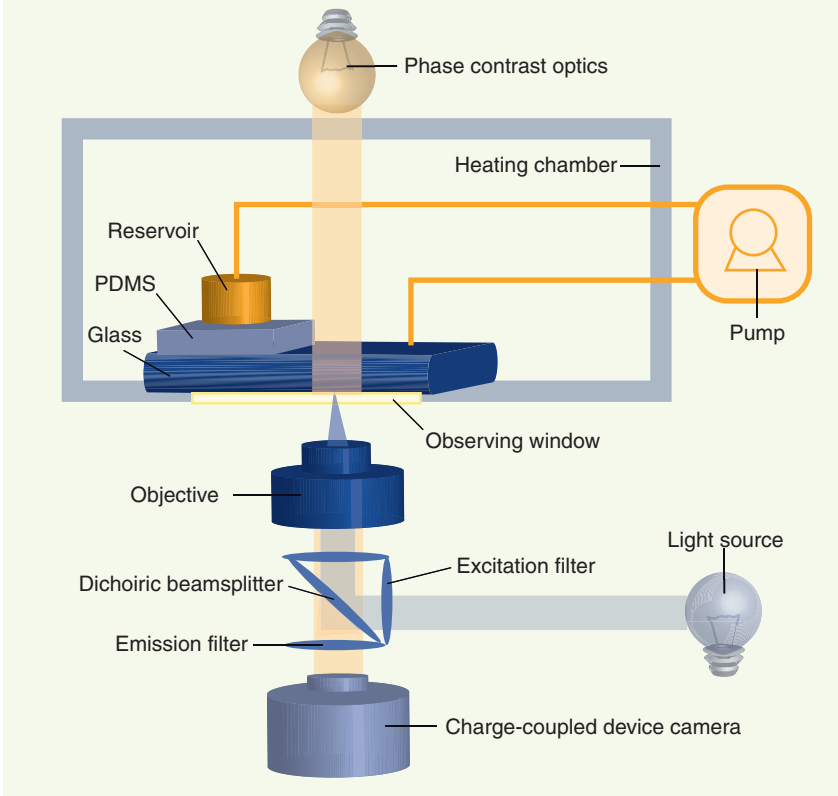

Figure 2. Microfluidic cell culture platform.

estimate the influence of the operating parameter, such as the height of the channel, a 1D unsteady computational model **(FIGURE 3A)** was established to simulate consumption of T/M complexes by the transfection occurred on the cell surface and diffusion of these complexes perpendicular to the cell surface (i.e., along the height of the system). With the coordinate systems defined as in **FIGURE 3A**, the diffusion equation describing the concentration of T/M as a function of position and time and its boundary and initial conditions is given by **EQUATIONS 1–4**:

$$\frac{\partial c}{\partial t} = D\frac{\partial^2 c}{\partial x^2} \quad \textbf{EQUATION 1}$$

$$D\frac{\partial c(0,t)}{\partial xx} - kc(0,t) = 0 \quad \textbf{EQUATION 2}$$

$$\frac{\partial c}{\partial x}(H,t) = 0 \quad \textbf{EQUATION 3}$$

$$c(x,0) = c_0 \quad \textbf{EQUATION 4}$$

where c is the concentration of T/M complexes, D is the diffusion constant, k is the first order rate constant, H is the height of the no-flow system, and c_0 is the initial T/M concentration. The boundary conditions, **EQUATIONS 2 & 3**, are derived from the mass balance on the top surface and the bottom surface where cells are located.

The partial differential equations (PDEs) can be solved by the method of separation of variables. Assume $c(x,t) = X(x) \cdot T(t)$, the PDE **(EQUATION 1)** and associated boundary **(EQUATIONS 2 & 3)** and initial **(EQUATION 4)** conditions are separated into ordinary differential equations (ODEs) for $X(x)$ and $T(t)$:

$$X''(x) + \lambda \cdot X(x) = 0 \quad \textbf{EQUATION 5}$$

$$T'(t) + \lambda D \cdot T(t) = 0 \quad \textbf{EQUATION 6}$$

$$D \cdot X'(0) - k \cdot X(0) = 0 \quad \textbf{EQUATION 7}$$

$$X'(H) = 0 \quad \textbf{EQUATION 8}$$

$$X(x) \cdot T(0) = c_0 \quad \textbf{EQUATION 9}$$

The solutions to **EQUATIONS 5 & 6** are:

$$X(x) = A_X \cos\beta x + B_X \sin\beta x \quad \textbf{EQUATION 10}$$

$$T(t) = AT e^{-\lambda D t} \quad \textbf{EQUATION 11}$$

where β = square root of λ. Along with β, the constants A_X, B_X and A_T are determined by **EQUATIONS 7–9**. Thus, an analytical solution to **EQUATION 1** in terms of a series expansion can be obtained:

$$c(x,t) = \sum_{n=1}^{\infty} C_n \cos\beta_n (H - x) e^{-\beta_n^2 D t} \quad \textbf{EQUATION 12}$$

$$C_n = \frac{c_0 \sin\beta_n H}{\frac{\beta_n H}{2} + \frac{\sin 2\beta_n H}{4}} \quad \textbf{EQUATION 13}$$

$$\cot(\beta_n H) = \frac{\beta_n H}{Da} \quad \textbf{QUATION 14}$$

where Da is Damköhler number, which estimates the relative importance of reaction kinetics and the mass transfer, and is defined in the no-flow system as the ratio of reaction rate to diffusion rate.

$$Da = \frac{k}{D/H} \quad \textbf{EQUATION 15}$$

For a given Da number, the T/M complexes concentration distribution along the height of the no-flow system was calculated by carrying out the series in **EQUATION 12** 1000 terms to ensure convergence.

■ Computational model for transfection in the flow system

In the experimental study of transfection under flow conditions, a channel with cavities **(FIGURE 3B)** was used. A 3D model can be applied to estimate the position dependence of the shear stress, which can potentially affect the transfection process. Another factor that governs the transfection efficiency is the spatial distribution

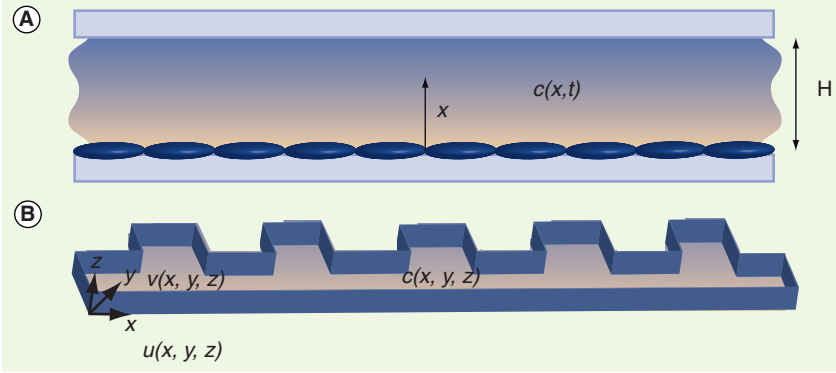

Figure 3. Computational models for simulating transfection in the cell culture systems. (A) Without flow. **(B)** With flow.

of the T/M complexes at the cell surface. Since the steady state is established almost immediately, a 3D steady computational model was used for the flow and mass transfer in this microchannel. It has been shown that the shear stress on cells in a microchannel with pressure-driven flow can be greater than that predicted in a cell-free microchannel and it is amplified by a factor inversely proportional to the ratio of the cell size to the height of the microchannel [27]. However, the small ratio of the cell thickness to the channel height (<0.1) in our experiments should create negligible perturbation on the shear stress; therefore, the computational model was based on a cell-free situation. Considering that the T/M complex has a density very close to that of cell culture media, the gravity is neglected and the velocity along the channel height is assumed to be zero in the model. Therefore, the governing equations and boundary conditions can be written as follows:

$$\frac{\partial u}{\partial x} + \frac{\partial v}{\partial y} = 0$$

EQUATION 16

$$\rho\left(u\frac{\partial u}{\partial x} + v\frac{\partial u}{\partial y}\right) = -\frac{\partial p}{\partial x} + \mu\left(\frac{\partial^2 u}{\partial x^2} + \frac{\partial^2 u}{\partial y^2} + \frac{\partial^2 u}{\partial z^2}\right)$$

EQUATION 17

$$\rho\left(u\frac{\partial v}{\partial x} + v\frac{\partial v}{\partial y}\right) = -\frac{\partial p}{\partial y} + \mu\left(\frac{\partial^2 v}{\partial x^2} + \frac{\partial^2 v}{\partial y^2} + \frac{\partial^2 v}{\partial z^2}\right)$$

EQUATION 18

$$u\frac{\partial c}{\partial x} + v\frac{\partial c}{\partial y} = D\left(\frac{\partial^2 c}{\partial x^2} + \frac{\partial^2 c}{\partial y^2} + \frac{\partial^2 c}{\partial z^2}\right)$$

EQUATION 19

$$u = u_0, v = 0, c = c_0$$

at inlet

EQUATION 20

$$u = v = 0$$

at all walls

EQUATION 21

$$\frac{\partial c}{\partial y} = 0$$

at side walls

EQUATION 22

$$\frac{\partial c}{\partial z} = 0$$

at top wall

EQUATION 23

$$D\frac{\partial c}{\partial z} = kc$$

at bottom wall

EQUATION 24

The coordinate axes are defined in FIGURE 3B. u is the velocity in the x direction, v is the velocity in the y direction, c is the concentration of T/M complexes, ρ is the fluid density, p is the fluid pressure, μ is the fluid viscosity, D is the diffusion constant, k is the first-order rate constant, and u_0 and c_0 are velocity and concentration at inlet. Since the advection dominates the mass transport in the flow system, here Da is given by:

$$Da = \frac{k}{u_0}$$

EQUATION 25

The numerical simulations based on the above model were performed with a commercial **computational fluid dynamic** (CFD) package CFD-ACE+ (CFD Research Corporation, Huntsville, AL, USA). From the numerical results of the velocity, the shear stress near the bottom cell surface τ_c was calculated based on Newton's law of viscosity:

$$\tau_c = -\mu\frac{\partial u}{\partial z}(z = 0)$$

EQUATION 26

Key term

Computational fluid dynamics: Uses numerical methods to analyze fluid dynamics problems.

Results & discussion

■ Molecular beacon design

There are several considerations in designing the molecular beacon for the current transfection study. First of all, the mRNA target of the molecular beacon should be constitutively expressed in the cell and the expression level of the mRNA target should be independent of the size and the flow of the cell culture system to elucidate their effects on the transfection efficiency. Second, the sequence of the molecular beacon should be designed such that the conformational change of the molecular beacon in the presence of the target mRNA is specific and thermodynamically favorable. Third, the nucleotides making up the molecular beacon should be chemically modified to enhance its stability against nuclease degradation. Based on the above considerations, a molecular beacon, Actin MB, was designed. Actin MB detects the human housekeeping β-actin mRNA, whose expression level was shown to be independent of the shear stress in the flow system [28,29]. A sequence of Actin MB was designed with the help of the thermodynamic prediction tool Mfold [30] and the Basic Local Alignment Search Tool (BLAST). 2′-*O*-methyl nucleotides, which have demonstrated resistance to the nuclease degradation [31,32], were adopted in the Actin MB.

To evaluate the design of Actin MB, characterization experiments were performed and the results are presented in **Figure 4**. The thermal denaturation profile **(Figure 4A)** indicates that the perfectly matched target (ACTB) can be differentiated from the single-base mismatched sequence (ACTB-1M) with the appropriately designed Actin MB. To examine the intracellular stability, Actin MB was transfected with JetPEI into 293T cells in a cell culture dish. Bright-field and fluorescence images were captured at different time points. **Figure 4B** shows the images taken at 5 and 28 h after the transfection. Despite the number of cells doubling in 1 day, the average intensity and local distribution of the fluorescence inside the cells remained almost the same. This suggests that Actin MB remains intact for at least 1 day. Otherwise, the cellular export of fluorophore following the degradation of oligonucleotides would lead to a decrease in the fluorescence intensity in the cell [17].

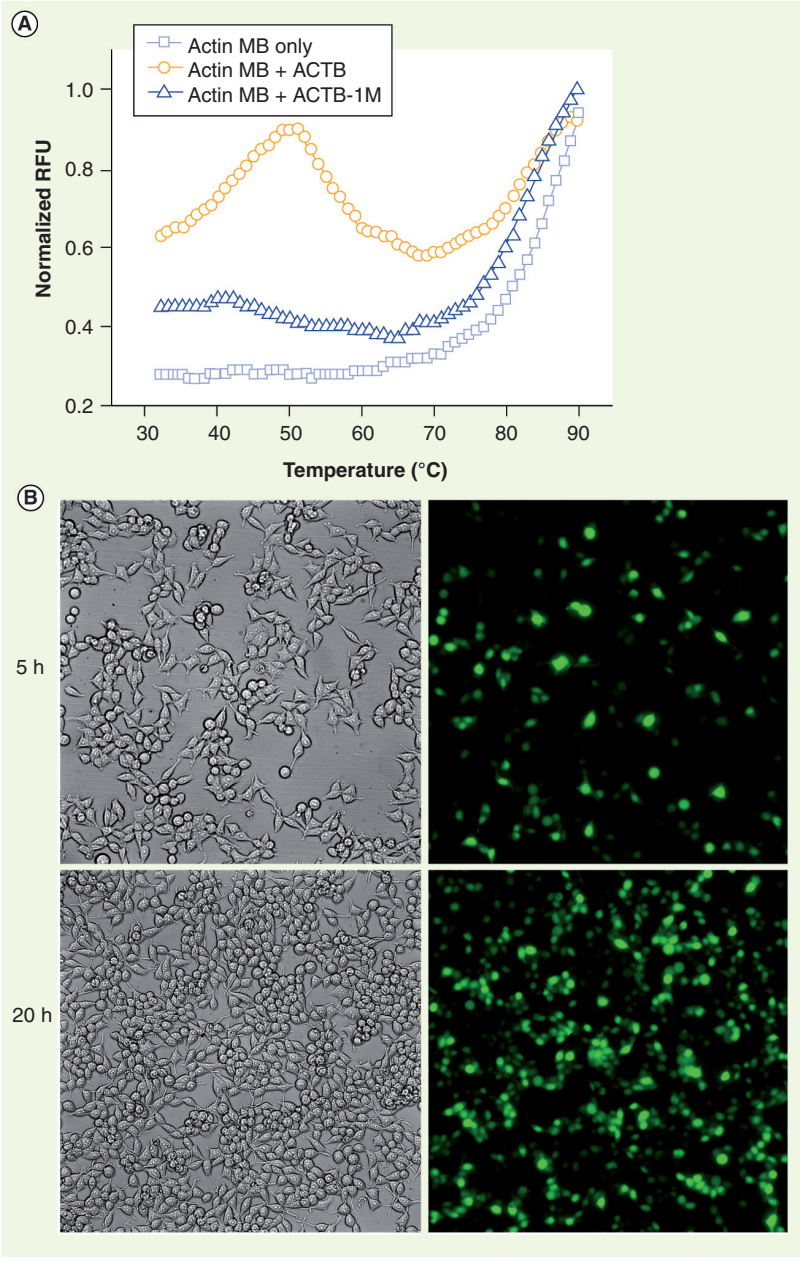

Figure 4. Thermal denaturation profiles. (A) Actin MB and the Actin MB/ACTB and Actin MB/ACTB-1M. **(B)** Stability of Actin MB in 293T cell.

■ Effects of the length–scale on the transfection

Transfection efficiency was compared between a no-flow microchannel and a 96-well plate. Due to the significantly different level of background fluorescence intensity in the 96-well plate and the microchannel, instead of the signal-to-background ratio, the percentage of cells that get transfected was used in the comparison. To determine whether a cell is transfected, a threshold signal-to-background ratio of 1.5 was defined. If a cell has a signal-to-background ratio greater than 1.5, the cell is counted as transfected. As expected, the transfection efficiency is highly sensitive to the concentration of the T/M complexes in both microchannels and 96-well plates. Interestingly, the transfection of the Actin MB into the 293T cells was generally less efficient in the no-flow microchannel compared with a 96-well plate **(Figure 5A)**. The heights of the microchannel and the solution in the 96-well plate were 30 µm and 3 mm. This results in a 100-fold difference in the surface-to-volume ratio. Two potential reasons for the reduced transfection efficiency, the reaction-diffusion kinetics and surface absorption, were further investigated. The 1D unsteady computational model was utilized to study the relative importance between the reaction kinetics and molecular diffusion. The computational results are presented in **Figure 5B & C**. It was found that the concentration profile of T/M in the 30-µm high microchannel was distinct for different *Da* numbers. Regardless of *Da* numbers, the concentration of T/M complexes at the cell surface in the microchannel was always lower than that in the 96-well plate. This can be explained by the fact that the effective number of T/M complexes available for each cell is smaller in the microchannel as a result of the small effective culture volume. Comparison of the experimental and computational results suggests that the reaction-diffusion kinetics plays an essential role in the overall transfection rate.

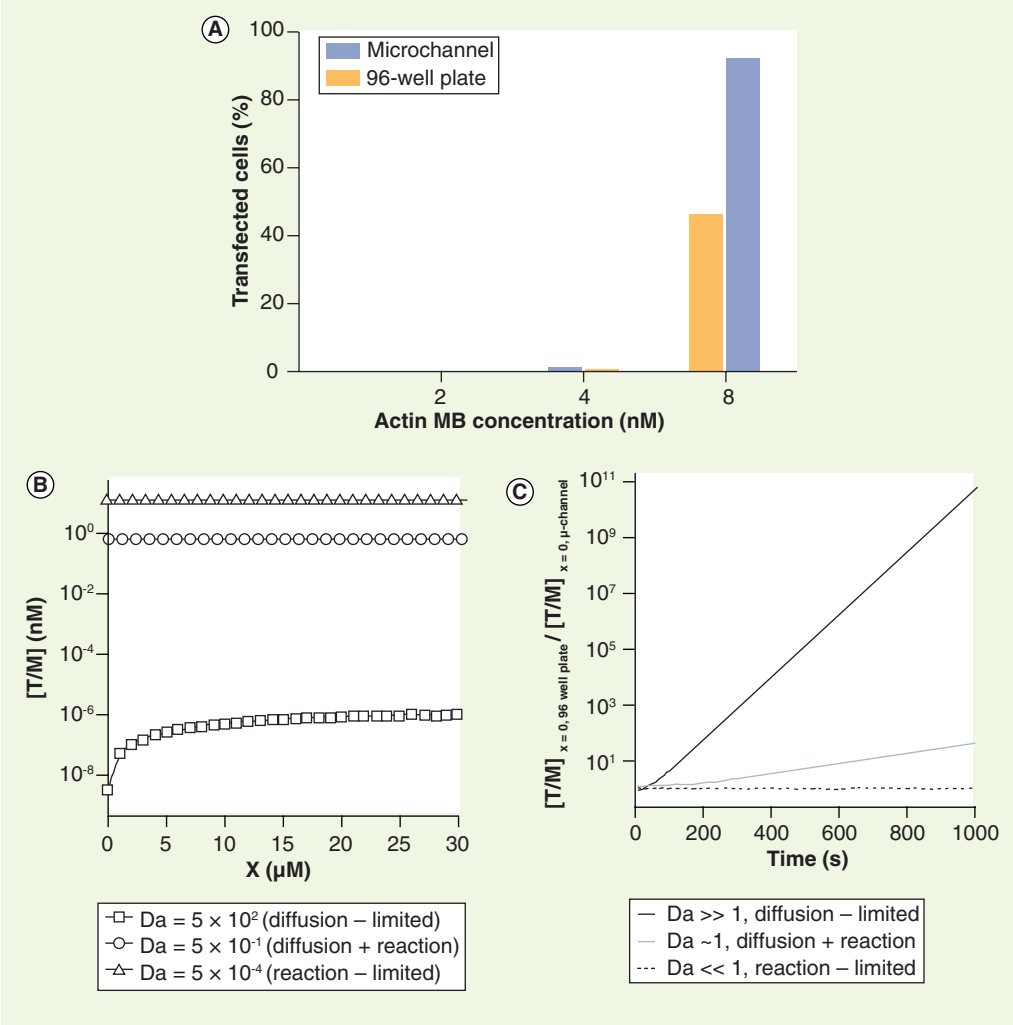

Figure 5. Transfection in static systems. (A) Experimental results on transfection of Actin MB into 293T cells inside a 30-μm high microchannel and a 96-well plate. **(B)** Computational results on concentration profiles of the 30-μm high microchannel at t = 10 min, c_o = 10 nM. **(C)** Computational results on the ratios of T/M complex concentration at the cell surface for the 96-well plate to that for the 30-μm high microchannel.
T/M: Transfection reagent/molecular beacon.

Considering the large surface-to-volume ratio in a microchannel, we had speculated that the absorption of T/M complexes to the channel surfaces could contribute to the reduced transfection efficiency observed in microchannels. Therefore, a control experiment was performed to test the extent of surface absorption. Green fluorophore-labeled Actin MB was first mixed with jetPEI-Fluor, a red fluorescent derivative of jetPEI, and then the mixture was introduced to a cell-free microchannel. After being incubated with the mixture for 30 min, the microchannel was flushed with the 1× PBS buffer and inspected with the fluorescence microscope. The fluorescence intensity observed in the microchannel was negligible compared with a fresh channel (data not shown). This suggests that the effect of surface absorption on the channel surface is insignificant in our experimental condition.

■ Flow effects on the intracellular delivery

To study the effects of the fluid flow on transfection in microfluidic systems, a microchannel with cavities was designed **(FIGURE 3B)**, which exposes the cells to different levels of shear stress and mass transfer rate simultaneously. CFD simulation based on the 3D steady computational model revealed the distribution of shear stress and T/M concentration at the cell surface, which are shown in **FIGURE 6A & B** respectively. The profile across the center of the cavity demonstrated that two

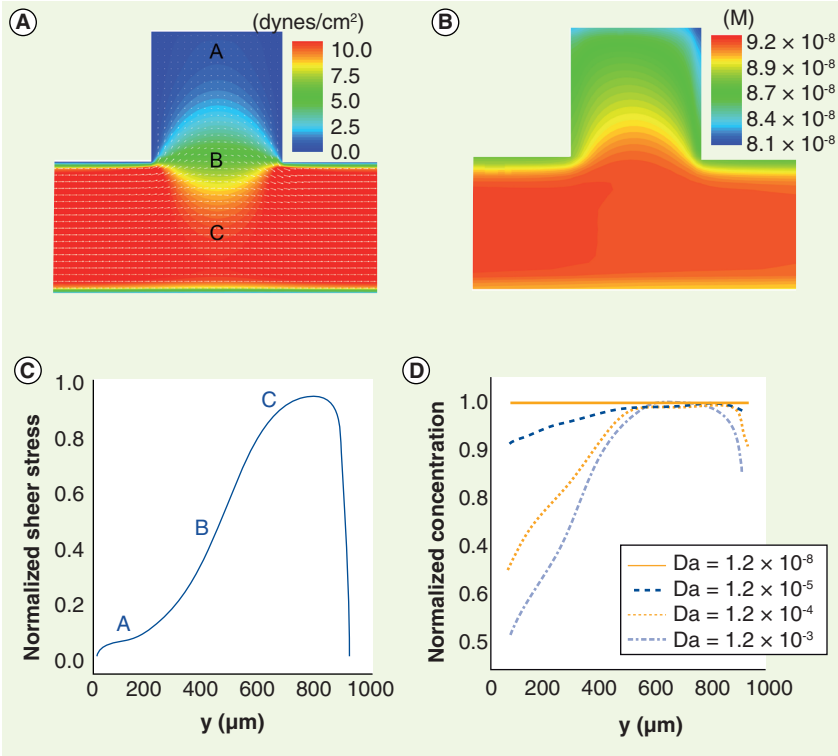

Figure 6. Computational fluid dynamics simulation results on transfection in the systems with flow. (A) Contour of shear stress at the cell surface with u_o = 0.014 m/s. **(B)** Contour of transfection reagent/molecular beacon complexes concentration at the cell surface with c_o = 100 nM, *Da* = 1.2e-5. **(C)** Profile of normalized shear stress along the center of a cavity. **(D)** Profiles of transfection reagent/molecular beacon complexes concentration along the center of a cavity for different *Da* numbers.

to three orders of magnitude difference in shear stress **(Figure 6C)** and 10–50% difference in T/M concentration **(Figure 6D)** at the cell surface can be achieved with this microchannel design.

In the experiment, transfection of Actin MB into HeLa cells was used as a model system for investigating the effect of fluid flow on the transfection efficiency. **Figures 7A, B & C** correspond to different positions in the microchannel, as shown in **Figure 6**, where cells experience different shear stress and mass transfer rate. An inverse dependence of transfection efficiency to shear stress and mass transfer rate was revealed in **Figure 7A**. The result of an unpaired **T-test** between the cell group A, B and C at 120 min ($p < 0.05$) indicates that the observed difference in transfection efficiency is statistically significant. Since the enhanced mass transfer facilitates transfection, the result indicates that shear stress can reduce transfection efficiency. While it has been well-established that shear stress can regulate gene expression in some cells (e.g., endothelial cells) *in vivo*, epithelial-like HeLa cells applied in the study do not respond to fluid shear stress *in vivo*. Our control experiment **(Figure 7B)** and previous studies [28,29] also indicate that expression of β-actin in HeLa cells is independent of the shear stress in our experimental condition. This further suggests the fluid flow in a microchannel can reduce the transfection efficiency.

The exact reason for the reduced transfection efficiency is unclear at the moment. The shear stress may directly interfere with the endocytosis mechanism or physically remove the T/M complexes from the cell membrane. If the T/M complexes are physically removed on the cell surface, the simplification of transfection as a pseudo first-order surface reaction in the computational modeling may no longer be valid and a more sophisticated model is required to accurately describe the transfection kinetics. Further studies will be required to confirm the mechanism of the reduced transfection efficiency. Nevertheless, our results will provide useful guidelines in designing microchannel molecular beacon transfection experiments for studying the gene expression dynamic in living cells. Appropriate design of the microchannel and the experimental conditions are required to maximize the transfection efficiency and utilize the potential of molecular beacons in single-cell gene-expression analysis.

Key term

T-test: Statistical test to assess whether the two groups are significantly different from each other.

Conclusion

In this article, the differences between transfection of molecular beacons in traditional cell culture systems and in microfluidic cell culture systems was investigated in two aspects: the effects of length–scale and fluid-flow. Both computational modeling and experimental studies were carried out. The reduced transfection efficiency in the no-flow microchannel, when compared with a 96-well plate, revealed that the reaction-diffusion kinetics of transfection is length–scale dependent. The reduced transfection efficiency under flow conditions suggested that although the fluid flow enhances mass transfer, the fluid shear stress can reduce the transfection efficiency to a greater extent. The results of this paper will provide insights on optimizing the design of microfluidic systems and the experimental conditions to achieve an efficient transfection of molecular beacon for studying the gene expression dynamic in living cells at the transcriptional level.

Future perspective

In this study, we investigated the transfection of molecular beacons inside microfluidic channels. The results are applicable to not

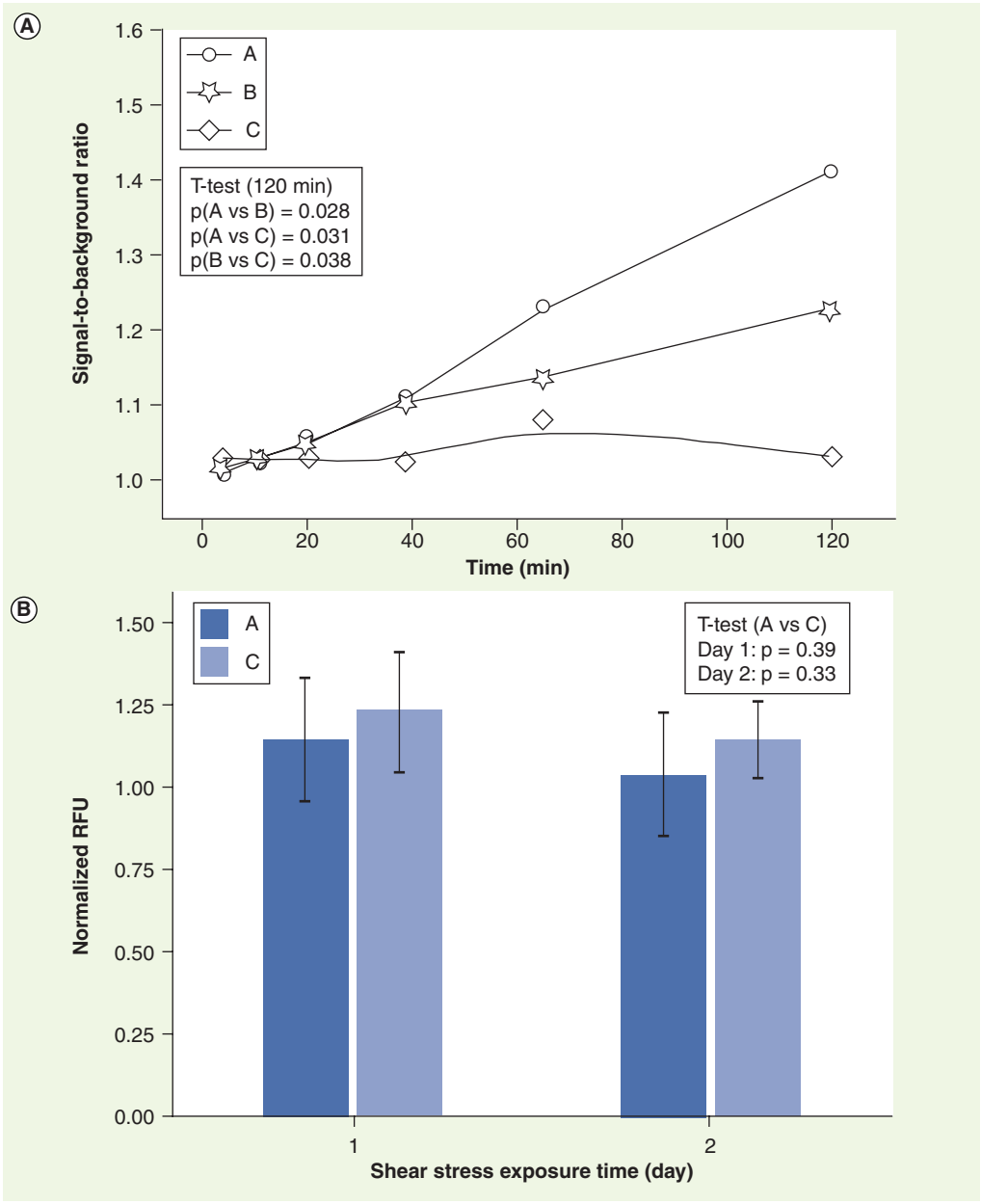

Figure 7. Experimental study of the transfection in the flow system. (A) Effects of flow on transfection efficiency. **(B)** Effects of flow on gene expression of β-actin. Error bars represent the standard error of the mean.

only molecular beacons that target mRNAs, but also other nucleic acid probes that target other intracellular molecules [33,34], With the parallel processing nature of microfluidics and the ability to integrate various physiochemical stimulation modularities into a microchannel, transfection of molecular probes in microfluidic cell culture systems will eventually provide highly sensitive and specific, yet simple, techniques for studying cellular gene regulatory mechanisms at both transcriptional and translational levels.

Ethical conduct of research

The authors state that they have obtained appropriate institutional review board approval or have followed the principles outlined in the Declaration of Helsinki for all human or animal experimental investigations. In addition, for investigations involving human subjects, informed consent has been obtained from the participants involved.

Financial & competing interests disclosure

This work was supported by the University of Miami (Provost's Research Awards), National Science Foundation (ECCS-0900899), Arizona Biomedical Research Commission

(0926) and the Prevent Cancer Foundation. The authors have no other relevant affiliations or financial involvement with any organization or entity with a financial interest in or financial conflict with the subject matter or materials discussed in the manuscript apart from those disclosed. No writing assistance was utilized in the production of this manuscript.

Executive summary

- A microfluidic platform, which allows long-term cell culture and continuous monitoring of the transfection of molecular beacons, has been developed.
- The differences between transfection of molecular beacons in traditional cell culture systems and in microfluidic cell culture systems were investigated systematically with a combination of computational and experimental methods.
- A study on the effects of the length scale on transfection revealed that scale-dependent reaction-diffusion kinetics play an essential role in the overall transfection rate and, therefore, should be taken into consideration when optimizing the transfection efficiency in the microfluidic system.
- A study of transfection under flow conditions suggests that the shear stress can reduce transfection efficiency. Therefore, caution should be used when trying to improve the transfection efficiency by enhancing the mass transfer with flow in the microfluidic system.

Bibliography

Papers of special note have been highlighted as:
- ▪ of interest
- ▪▪ of considerable interest

1 Stark GR, Kerr IM, Williams BRG, Silverman RH, Schreiber RD. How cells respond to interferons. *Annu. Rev. Biochem.* 67, 227–264 (1998).

2 Muller H, Bracken AP, Vernell R *et al.* E2fs regulate the expression of genes involved in differentiation, development, proliferation, and apoptosis. *Genes Dev.* 15(3), 267–285 (2001).

3 Nelson DE, Ihekwaba AEC, Elliott M *et al.* Oscillations in NF-κB signaling control the dynamics of gene expression. *Science* 306(5296), 704–708 (2004).

4 Elowitz MB, Leibler S. A synthetic oscillatory network of transcriptional regulators. *Nature* 403(6767), 335–338 (2000).

5 Tyagi S, Kramer FR. Molecular beacons: probes that fluoresce upon hybridization. *Nat. Biotechnol.* 14(3), 303–308 (1996).

6 Walker GM, Zeringue HC, Beebe DJ. Microenvironment design considerations for cellular scale studies. *Lab Chip* 4(2), 91–97 (2004).

▪▪ **Discusses the various factors that need to be taken into consideration when performing cellular studies at the microscale.**

7 Dertinger SKW, Chiu DT, Jeon NL, Whitesides GM. Generation of gradients having complex shapes using microfluidic networks. *Anal Chem.* 73(6), 1240–1246 (2001).

8 Jeon NL, Dertinger SKW, Chiu DT, Choi IS, Stroock AD, Whitesides GM. Generation of solution and surface gradients using microfluidic systems. *Langmuir* 16(22), 8311–8316 (2000).

9 Marras SAE, Kramer FR, Tyagi S. Efficiencies of fluorescence resonance energy transfer and contact-mediated quenching in oligonucleotide probes. *Nucleic Acids Res.* 30(21), 8 (2002).

10 Tyagi S, Bratu DP, Kramer FR. Multicolor molecular beacons for allele discrimination. *Nat. Biotechnol.* 16(1), 49–53 (1998).

11 Santangelo P, Nitin N, Bao G. Nanostructured probes for RNA detection in living cells. *Ann. Biomed. Eng.* 34(1), 39–50 (2006).

12 Yeh HC, Chao SY, Ho YP, Wang TH. Single-molecule detection and probe strategies for rapid and ultrasensitive genomic detection. *Curr. Pharm. Biotechnol.* 6(6), 453–461 (2005).

13 Abravaya K, Huff J, Marshall R *et al.* Molecular beacons as diagnostic tools: technology and applications. *Clin. Chem. Lab. Med.* 41(4), 468–474 (2003).

14 Wong PK, Yu FQ, Shahangian A, Cheng GH, Sun R, Ho CM. Closed-loop control of cellular functions using combinatory drugs guided by a stochastic search algorithm. *Proc. Natl Acad. Sci. USA* 105(13), 5105–5110 (2008).

15 Chen CH, Lu Y, Sin ML *et al.* Antimicrobial susceptibility testing using high surface-to-volume ratio microchannels. *Anal. Chem.* 82(3), 1012–1019 (2010).

16 Kim D-H, Wong PK, Park J, Levchenko A, Sun Y. Microengineered platforms for cell mechanobiology. *Annu. Rev. Biomed. Eng* 11, 203–233 (2009).

17 Leonetti JP, Mechti N, Degols G, Gagnor C, Lebleu B. Intracellular-distribution of microinjected antisense oligonucleotides. *Proc. Natl Acad. Sci. USA* 88(7), 2702–2706 (1991).

18 Sokol DL, Zhang XL, Lu PZ, Gewitz AM. Real time detection of DNA RNA hybridization in living cells. *Proc. Natl Acad. Sci. USA* 95(20), 11538–11543 (1998).

19 Tsong TY. Electroporation of cell membranes. *Biophys. J.* 60(2), 297–306 (1991).

20 Chen AK, Behlke MA, Tsourkas A. Efficient cytosolic delivery of molecular beacon conjugates and flow cytometric analysis of target RNA. *Nucleic Acids Res.* 36(12), 10 (2008).

▪ **Compares several different methods for intracellular delivery of molecular beacons.**

21 Tang MX, Redemann CT, Szoka FC. *In vitro* gene delivery by degraded polyamidoamine dendrimers. *Bioconjug. Chem.* 7(6), 703–714 (1996).

22 Suh J, Wirtz D, Hanes J. Efficient active transport of gene nanocarriers to the cell nucleus. *Proc. Natl Acad. Sci. USA* 100(7), 3878–3882 (2003).

23 Nitin N, Santangelo PJ, Kim G, Nie SM, Bao G. Peptide-linked molecular beacons for efficient delivery and rapid mRNA detection in living cells. *Nucleic Acids Res.* 32(6), (2004).

24 Pipkorn R, Waldeck W, Braun K. Synthesis and application of functional peptides as cell nucleus-directed molecules in the treatment of malignant diseases. *J. Mol. Recognit.* 16(5), 240–247 (2003).

25 Boussif O, Lezoualch F, Zanta MA *et al.* A versatile vector for gene and oligonucleotide transfer into cells in culture and *in vivo* – polyethylenimine. *Proc. Natl Acad. Sci. USA* 92(16), 7297–7301 (1995).

26 Chesnoy S, Huang L. Structure and function of lipid–DNA complexes for gene delivery. *Annu. Rev. Biophys Biomol. Struct.* 29, 27–47 (2000).

27 Gaver DP, Kute SM. A theoretical model study of the influence of fluid stresses on a cell adhering to a microchannel wall. *Biophys. J.* 75(2), 721–733 (1998).

28 Braddock M, Schwachtgen JL, Houston P, Dickson MC, Lee MJ, Campbell CJ. Fluid shear stress modulation of gene expression in endothelial cells. *News Physiol. Sci.* 13, 241–246 (1998).

29 Schwachtgen JL, Houston P, Campbell C, Sukhatme V, Braddock M. Fluid shear stress activation of egr-1 transcription in cultured human endothelial and epithelial cells is mediated via the extracellular signal-related kinase 1/2 mitogen-activated protein kinase pathway. *J. Clin. Invest.* 101(11), 2540–2549 (1998).

30 Zuker M, Mathews DH, Turner DH. Algorithms and thermodynamics for RNA secondary structure prediction: a practical guide. In: *RNA Biochemistry and Biotechnology*. Barciszewski J, Clark BFC (Eds). Kluwer Academic Publishers, Berlin, Germany, 11–44 (1999).

31 Molenaar C, Marras SA, Slats JCM *et al.* Linear 2′ *O*-methyl RNA probes for the visualization of RNA in living cells. *Nucleic Acids Res.* 29(17), e89 (2001).

32 Bratu DP, Cha BJ, Mhlanga MM, Kramer FR, Tyagi S. Visualizing the distribution and transport of mRNAs in living cells. *Proc. Natl Acad. Sci. USA* 100(23), 13308–13313 (2003).

33 Li N, Ho CM. Aptamer-based optical probes with separated molecular recognition and signal transduction modules. *J. Am. Chem. Soc.* 130(8), 2380–2381 (2008).

34 Wang ZH, Gidwani V, Zhang DD, Wong PK. Separation-free detection of nuclear factor κ b with double-stranded molecular probes. *Analyst* 133(8), 998–1000 (2008).